Dalton Transactions

ROYAL SOCIETY OF CHEMISTRY

PAPER

View Article Online
View Journal | View Issue

Cite this: *Dalton Trans.*, 2025, **54**, 5143

Heteroleptic phenoxyimino tin(II) bis(trimethylsilyl) amides for the synthesis of poly(diester-*alt*-ethers) from cyclohexene oxide and succinic anhydride†

Trinity Quek, Phongnarin Chumsaeng and Khamphee Phomphrai *

The search for biodegradable polyesters with tunable physical properties has gone beyond the ring-opening polymerisation of cyclic esters to the copolymerisation of epoxides and cyclic anhydrides. Tin(II) complexes are active for the reaction between cyclohexene oxide and succinic anhydride monomers to produce a psuedo-periodic polymer: multiple epoxide insertions occur for every cyclic anhydride. In this paper, six heteroleptic phenoxyimino tin(II) bis(trimethylsilyl)amide complexes were synthesised and characterised by single crystal X-ray diffraction. When used as catalysts for the polymerisation of cyclohexene oxide and succinic anhydride under neat conditions at 110 °C, an average of four cyclohexene oxide molecules were incorporated for every succinic anhydride, while the proportion of pure polyester $(AB)_n$ units was low (less than 8.5%). To obtain evidence for the average numbers of cyclohexene oxides inserted between each succinic anhydride, polymer samples were hydrolysed at the ester linkages and the resulting fragments were analysed by electro-spray ionisation mass spectrometry. When solvents such as toluene or tetrahydrofuran were added to the polymerisation system, less epoxide was incorporated. Tetrahydrofuran could also be incorporated into the polymer at a ratio of two-fifths with respect to succinic anhydride.

Received 21st December 2024,
Accepted 21st February 2025

DOI: 10.1039/d4dt03514c

rsc.li/dalton

Introduction

The copolymerisation of epoxides and cyclic anhydrides offers several advantages in the search for polymers which are degradable in the natural environment, since ester linkages are formed during polymerisation.[1,2] Most commonly used polymers do not decompose easily and polyesters are one of the prime candidates for polymers which can be hydrolytically[3] or enzymatically[4] degraded. This strategy of utilising two large categories of monomers potentially allows for a multitude of polymer products, as well as several different polymer architectures, as shown in Fig. 1. The various architectures also create opportunities for the composition of the resulting polymer to be tuned, whether due to monomer properties or resulting linkages. Polymers with both ester and ether groups offer different properties from a pure polyester.[5–7] Additionally, the glass-transition temperature (T_g) of the resulting polymer can be tuned by mixing and matching of the structural rigidity or flexibility of cyclic anhydride or epoxide monomers.[8,9]

Concerning the alternating co-polymer type, much success has been attained in the quest for a pure polyester.[10] In 2007, this was achieved using β-diiminate zinc complexes.[11] Interestingly, one report found Cr, Co, and Al salen complexes to be effective in solution polymerisation, but produced poly-

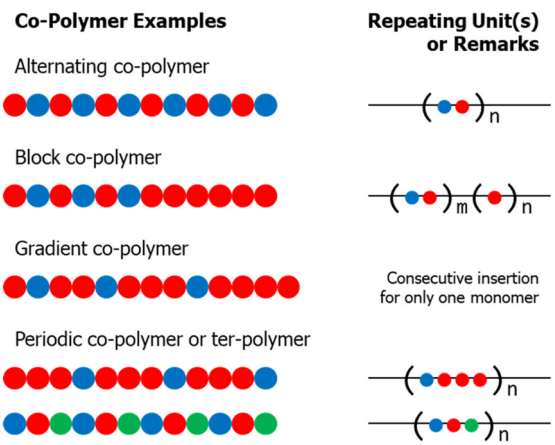

Fig. 1 Depictions of various types of linear co-polymers: block, gradient, alternating, and periodic.

Department of Materials Science and Engineering, School of Molecular Science and Engineering, Vidyasirimedhi Institute of Science and Technology (VISTEC), 555 Moo 1 Payupnai, Wangchan, Rayong 21210, Thailand. E-mail: khamphee.p@vistec.ac.th

†Electronic supplementary information (ESI) available: NMR spectra, method for parameter calculation, ESI and MALDI-TOF mass spectrometry. CCDC 2378870–2378875. For ESI and crystallographic data in CIF or other electronic format see DOI: **https://doi.org/10.1039/d4dt03514c**

esters with ether content in bulk polymerisation.[12] Zhao and coworkers copolymerised phthalic anhydride with ethylene/propylene oxide using a metal-free catalyst that could insert consecutive epoxides to produce a sort of gradient between alternating and polyether segments.[13] A di-block polyester–polyether product could also be achieved by tuning the catalyst compositions. Gradient and block co-polymers are frequently the result of unsuccessful attempts at producing a pure alternating polyester. As such, it is common for ether content to be reported, in the pursuit of polymerisation conditions yielding near-zero ether content and perfectly alternating copolymers. Periodic poly(ester-*alt*-ether)s, in contrast, have significant ether content without alternating segments. Periodic polymers are relatively uncommon, and periodic polyesters are rarer yet. Nonetheless, there have been a few studies featuring periodic or pseudo-periodic polyesters. The synthesis of an ether–ester–ester periodic polymer was reported as far back as 1973, when tetrahydrofuran (THF) solvent was incorporated into the copolymerisation of epichlorohydrin and phthalic anhydride in the presence of triisobutylaluminum catalyst.[14] The researcher postulated an ABC–ABC–ABC periodic polymer. In 2012, an ABB–ABB–ABB periodic polymer was reported with two molecules of THF incorporated for every molecule of glutaric anhydride.[15] Molecular weights of 12 kDa (polydispersity = 1.97) after 8 h at 50 °C were achieved using the organic catalyst nonafluorobutane sulfonimide, although only polyesters were obtained at 120 °C.

Altogether, periodic polymers produced through multiple insertion of epoxide during copolymerisation is a relatively recent strategy for block-polyethers with polyester segments. Most recently, our group reported that tin(II) octoate is able to incorporate THF into the AB_x polymer.[16] This concurs with the observations of Kerr and Williams using a Zr(IV) catalyst.[17,18] From a report by Chidara *et al.*, triethylborane was shown to control anhydride insertion during polymerisation with ethylene oxide to produce gradient or periodic polymers.[19] Meanwhile, Kanazawa and Aoshima published a different type of ABC polymer with both ester and ether linkages. Their system used 3-alkoxyphthalides, epoxides, and vinyl monomers.[20] They introduced the term 'pseudo-periodic' to accurately describe the polymer architecture and also used electrospray ionisation mass spectrometry (ESI-MS) to analyse the product.

While several metal complexes have been reported for the ring-opening polymerisation (ROCOP) of cyclic anhydrides and epoxides, tin(II) complexes appeared to be one of the most promising candidates since tin(II) metal tends to promote multiple insertions of epoxides. Our group previously reported that a tin(II) catalyst was able to cause double insertion of cyclohexene oxide such that polyether linkages occur somewhat regularly along the polymer chain.[21] Williams and coworkers also observed similar behaviour when propylene oxide is copolymerised with maleic anhydride in the presence of tin (II) alkoxides.[22] Other examples of well-defined tin(II) initiators for polymerisations of cyclic esters include tin(II) aminophenolates[23] and tin(II) amidinates[24,25] for the polymerisation of lactide and lactone. In 2009, phenoxyimine Sn(II) complexes with dimethylamide were reported – one of them curiously displayed the result of the amide attacking the imino group.[26,27]

While several homoleptic tin(II) complexes supported by simple Schiff-base phenoxyimine ligands were reported such as bis(phenoxyimine) tin(II),[28] there has been only limited example of the heteroleptic phenoxyimine tin(II) complex.[26] Very bulky substituents were deployed to overcome the kinetic instability which could otherwise cause ligand scrambling to the bis(phenoxyimine) tin(II) complexes. In this study, we found a method to synthesise heteroleptic tin(II) amides supported by phenoxyimine ligands with varying steric and electronic contributions. They were shown to be active for the ROCOP of succinic anhydride and cyclohexene oxide leading to a periodic co-polymer as shown in Fig. 1.

Results and discussion

Sn(II) complex synthesis

Simple Schiff base ligand precursors were selected due to the ease of ligand synthesis and property modification as shown in Scheme 1. Taking advantage of the modular synthesis, the phenoxy-imine ligands for the Sn(II) complexes were designed with a tunable aromatic ring. The ligand precursors for complexes **1–3** feature increasing steric hindrance on the complexes (R_1 = H, Me, ^{i}Pr for **1–3**, respectively), while the ligand precursors for complexes **4–6** vary the electronic effects on the tin atom (R_2 = CF_3, ^{t}Bu, OMe for **4–6**, respectively).

The synthesis of heteroleptic tin complexes was attempted by reacting a 1 : 1 ratio of $Sn[N(SiMe_3)_2]_2$ and the ligand precursors as outlined in Scheme 1. Initial NMR-scale attempts in benzene-d_6 proved that the desired complexes were successfully formed in solution. However, complications arose during workup when directly applying a vacuum to remove both solvent and by-product hexamethyldisilazane (HMDS) failed to leave behind pure complexes. Homoleptic complex as well as free ligand were detected, reflecting the difficult experiences by an aforementioned report.[26] We found that exposure to vacuum seemed to promote decomposition. Johnson and coworkers[29] also reported some difficulty in isolating pure heteroleptic mono(dimethylamido) Sn(II) compounds and instead obtained a product mixture largely comprised of the homoleptic bis-pyrrolide. Nonetheless, the team was later able to syn-

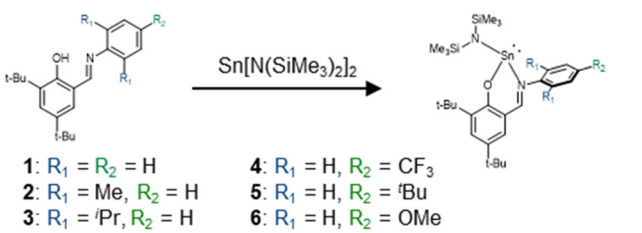

Scheme 1 Synthesis of heteroleptic tin(II) complexes from ligand precursors with variation of steric and electronic properties.

thesise heteroleptic Sn(II) aminoalkoxide compounds as major products.[30]

After several attempts, we successfully devised the following method for product isolation. First, $Sn[N(SiMe_3)_2]_2$ was reacted with the ligand in a 1 : 1 ratio using hexane as a solvent due to its low boiling point. The reaction was completed in 2 h. After that, most of the hexane solvent was removed under vacuum such that the product precipitated before all the solvent was completely removed. The product mixture was subsequently washed with cold hexane to remove the HMDS. Afterwards, remaining volatiles can be removed under vacuum. Moderate yields (36–69%) were obtained probably affected by washing with hexane, but the heteroleptic complexes **1–6** were now obtained in high purity. Once the heteroleptic complexes were isolated in pure form, they are rather stable in both solution and solid forms. The molar ratio of ligand and tin bis(trimethylsilyl)amide in the complexes is 1 : 1 by ^{1}H NMR confirming the existence of heteroleptic L–Sn–$N(SiMe_3)_2$. It is worth mentioning that this synthesis method is successful even with the complex having the least steric hindrance as in complex **1** ($R_1 = R_2 = H$). Based on these results, it is apparent that the complexes are unstable under negative pressure in the presence of HMDS. We do not know the mechanism behind the decomposition yet, but we suspect that the NH moieties in the HMDS could facilitate in the ligand redistribution.

The complexes were crystallised and characterised by single-crystal X-ray crystallography. All complexes were shown to be heteroleptic monomeric species as shown in Fig. 2 with selected bond distances and angles in Table 1. The crystal class of **1–2** were triclinic, with a space group of $P\bar{1}$. The crystal

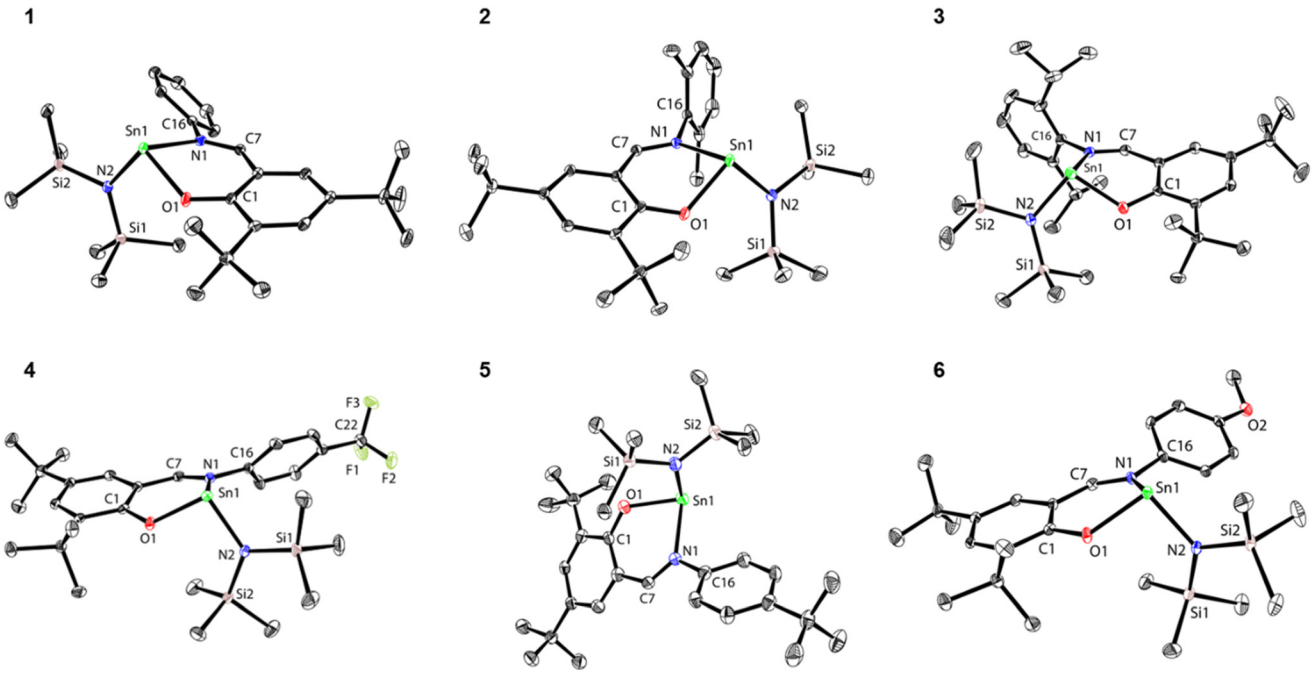

Fig. 2 Molecular structures (ORTEP) of complexes **1–6**. Ellipsoids are drawn at 50% probability level. Hydrogen atoms are omitted for clarity.

Table 1 Selected bond distances and angles for complexes **1–6**

Complex	1	2	3	4[a]	5	6
Selected bond distances (Å)						
Sn1 O1	2.084(1)	2.089(1)	2.070(1)	2.075(1), 2.079(1)	2.076(3)	2.082(1)
Sn1 N1	2.319(2)	2.333(1)	2.355(1)	2.311(2), 2.330(2)	2.308(3)	2.295(2)
Sn1 N2	2.095(2)	2.107(1)	2.095(1)	2.092(2), 2.089(2)	2.100(3)	2.107(2)
N1 C16	1.436(2)	1.438(1)	1.441(1)	1.426(2), 1.424(2)	1.429(5)	1.431(3)
N1 C7	1.297(2)	1.289 (1)	1.289(1)	1.293(3), 1.294(3)	1.296(5)	1.296(3)
Selected bond angles (°)						
O1 Sn1 N1	81.41(6)	79.92(3)	80.61(3)	81.19(5), 80.19(5)	81.46(11)	82.96(5)
O1 Sn1 N2	97.65(6)	95.60(3)	95.79(3)	96.46(6), 95.71(6)	95.57(12)	96.24(6)
N2 Sn1 N1	93.81(6)	99.19(3)	98.98(3)	94.56(6), 95.46(6)	95.60(12)	99.60(6)
Sum of angles	272.9	274.7	275.4	272.2, 271.4	272.6	278.8
Torsion[b]	35.9(3)	84.1(1)	109.5(1)	44.2(3), 37.2(3)	37.8(5)	39.6(3)

[a] Complex **4** has two molecules per unit cell – the data for both are given. [b] The torsional angles between the C=N imine group to the substituted aniline ring.

class of **3–6** were monoclinic, **3** has a space group of *P*21/*n* and the others *P*21/*c*. **4** is also noted to have two molecules per unit cell, one of which features the common CF_3 disorder. From the molecular structures of the complexes, we clearly see the effect of a stereo-active electron lone pair commonly found in tin(II) compounds. The tin(II) atom coordinates to the phenolic oxygen as well as the nitrogen atoms, in a trigonal pyramidal geometry. All bond angles around the tin(II) atoms were below 100°. This is due to the repulsion of the 'inert' lone pair of tin which actually has antibonding character.[31] The geometries around both N atoms were almost trigonal planar, implying that they do not have available stereo-active lone pair electrons, unlike the lone pairs of the tin and oxygen atoms. The Sn–O bond distances range 2.070–2.089 Å, while the distance between Sn and N_{amide} ranges 2.089–2.107 Å. The distance between Sn and N_{imine} ranges from 2.295 Å to 2.355 Å, much longer than the Sn–N_{amide} distances. This indicates that the N_{imine} atom coordinates datively, although steric hindrance may also influence the bond distances to some extent.

The tortional angles between C=N imine and the substituted aniline ring can be divided into two groups. The tortional angles less than 45° were found in complexes **1**, **4–6** ranging from 35.9–44.2°. These complexes do not have any substituents at the *ortho* positions. Therefore, the aniline rings are prone to rotate around the C_{ipso}–N_{imine} bond (*e.g.* N1–C16 in complex **1**). A close inspection of the ^{1}H NMR of these complexes also reveals equivalent proton signals of the *ortho* or *meta* positions indicating that there is a fast rotation around the C_{ipso}–N_{imine} bond on NMR timescale. The second group having much larger tortional angles was found in complexes **2** (84.1°, R_1 = Me) and **3** (109.5°, R_1 = ^{i}Pr). Large tortional angles suggest that there is considerable steric hindrance imposed by the *ortho* substituents. From ^{1}H NMR, complexes **2** and **3** revealed two inequivalent sets of R_1 and two sets of protons at the *meta* position indicating that there is no free rotation around the C_{ipso}–N_{imine} bond (*i.e.* N1–C16 bond) in complexes **2–3**.

Copolymerisation of succinic anhydride and cyclohexene oxide

Complexes **1–6** were used as catalysts for the copolymerisation between cyclohexene oxide (CHO) and succinic acid (SA). As higher reaction temperatures are the norm for tin catalysts, CHO (boiling point 130 °C) was chosen as a model monomer for this ROCOP reaction. CHO was added in excess to facilitate faster polymerisations and to serve as a solvent for the copolymerisation. SA, as a simple cyclic anhydride with potentially green sources was also used. Briefly, a polymerisation flask was charged with the catalyst, CHO, and SA under a nitrogen atmosphere in a glovebox. SA dissolved as the mixture was heated to 110 °C. The polymerisations were terminated when it became too viscous to be stirred. The polymer product was then checked for conversion which is around 80–90% conversion of SA and isolated through precipitation in cold methanol.

An NMR spectra of a representative polymer product is shown in Fig. 3. It is immediately apparent that the signal **a** seen in pure alternating polyesters is very small when compared to **b**, indicating that most of time, the first CHO molecule inserted after an SA molecule is not followed by an SA molecule, but by another CHO. CHO protons which are next to an ether group are indicated as **c**. The ratio of CHO incorporation to SA can be determined by summing up the signals from CHO (**a–c**, 2H) and dividing by half the signal **d** (4H) from SA (see ESI†). For clarity, this monomer incorporation ratio will be referred to as the B/A ratio (equals to (**a** + **b** + **c**)/(**d**/2)). Using catalysts **1–6**, the polymer products all featured a high amount of epoxide incorporation, with B/A ratios of about 4 (Table 2, entries 1–6). This is an increase from our previous work featuring a tin(II) catalyst and CHO 'mis-insertion' with a B/A ratio of about 2.[21] When the B/A ratio was monitored with time as shown in Fig. 4, a higher proportion of epoxides were already observed from the start of the reaction suggesting that the higher epoxide incorporation was not due to formation of block polyethers. DOSY NMR further confirmed that the product consisted of only one type of polymer (Fig. S16†). Therefore, it could be construed as a polymer consisting of diester linkages alternating with an average of three ether linkages (AB_n, average n = 4). The tin(II) complexes appeared to promote multiple insertions of epoxides as seen earlier,[16,21] rather than the alternate insertions. It could be due to the large metal size that enhanced consecutive insertions of epoxides through longer M–OR bond. Similar effect was also observed by Williams in Zr(IV) complex.[17] Our proposed polymerisation mechanism shown in Scheme S1 in ESI† is in agreement with previous report.[17] After the LSn–OR attacks SA monomer, the Sn carboxylate was obtained. The Sn carboxylate subsequently inserts CHO giving the ring-opened Sn–OR moieties again. At this point, several insertions of CHO may take place giving multiple insertions of CHO units followed by insertion of SA to complete the catalytic cycle.

The polymerisation appears to have an induction period of around 20–30 minutes due to a slow initiation commonly

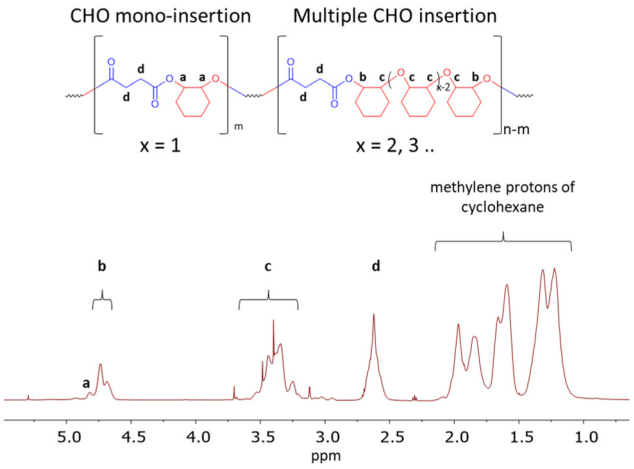

Fig. 3 ^{1}H NMR spectra (600 MHz, $CDCl_3$, 30 °C) of the copolymer from SA and CHO using the cat./SA/CHO molar ratio of 1 : 200 : 1000 (Table 2, entry 3).

Table 2 Copolymerisation of "A" succinic anhydride (SA) and "B" cyclohexene oxide (CHO) at 110 °C

Entry	Complex	Loading ratio Cat. : SA : CHO	Time (h)	TOF of SA (h^{-1})	Degree of polymerisation A : B[a]	B/A ratio[a]	$(AB)_n$ fraction[a] (%)	M_n[b] (g mol^{-1})	$Đ$[b]	T_g[c] (°C)
1	**1**	1 : 200 : 1000	4	45	179 : 788	4.40	3.9	4300	1.50	53.5
2	**2**	1 : 200 : 1000	4	42	169 : 665	3.94	4.3	3500	1.72	43.7
3	**3**	1 : 200 : 1000	2.5	67	167 : 693	4.14	8.5	4400	1.57	49.3
4	**4**	1 : 200 : 1000	3	60	179 : 754	4.22	7.1	4600	1.84	47.4
5	**5**	1 : 200 : 1000	4	45	178 : 691	3.88	4.9	4900	1.60	52.7
6	**6**	1 : 200 : 1000	4	43	173 : 685	3.95	5.5	4400	1.62	55.3
7	**3**	1 : 100 : 1000	3	61	91 : 410	4.49	4.5	3600	2.14	52.9
8	**3**	1 : 400 : 1000	2	56	222 : 941	4.24	7.1	3500	1.49	59.4
9	**3**	1 : 100 : 500[d]	6	31	93 : 287	3.09	3.0	4100	1.63	48.6

Ratios are in molar equivalent. [a] Calculated from NMR spectroscopy, details in the ESI.† [b] Determined by GPC. [c] Determined by DSC. [d] Toluene was added equal in volume to CHO.

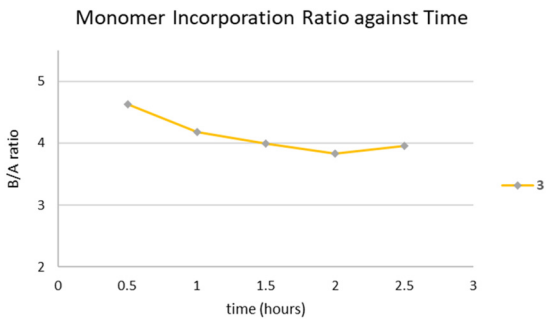

Fig. 4 The B/A ratio recorded at different time for the copolymerisation described in Table 2, entry 3.

found in tin(II) catalysts;[32] the plots (Fig. S18†) do not pass through the origin when extrapolated. The induction period has been attributed to higher initial activation energies, implicating the inert lone pair as a major source of steric hindrance.[33] In our case, HMDS would also impose steric demands for the first few monomer insertions before the growing polymer chain positions it further away. Amongst complexes **1–3** which feature ligands with varying steric effects, **3** proved to be the most active catalyst, completing the reaction in 2.5 h. Therefore, the bulky diisopropyl groups generating steric stress favours the catalytic activity. As for complexes **4–6** featuring ligands with varying electronic effects, **4**, with a CF_3 electron-withdrawing group, is the most active catalyst in this group possibly due to the enhanced Lewis acidity of the metal center giving a better monomer coordination. All complexes produced copolymer with low alternating $(AB)_n$ fractions (3.9–8.5%).

Complex **3**, as the most active complex in this study, was then used in a series of experiments to determine the impact of monomer concentration and other variables on the product polymer. The results are summarised in Table 2. When the amount of SA introduced at the start of the reaction was reduced from 200 to 100 equiv. (entries 3 and 7), the DP of CHO dropped from 167 to 91. When the amount of SA was increased to 400 equiv. (entry 8), the DP of SA could only go to 222 since CHO almost went to completion. In all cases, the B/A ratios (4.14–4.49) are not significantly different. This implies that the insertion of CHO is not statistical, and the high B/A ratio is due to the catalyst rather than monomer concentration. The polymers produced by complex **3** had glass transition temperatures ranging 49–59 °C, higher than the T_g of perfectly alternating poly(CHO-*alt*-SA) which has been reported as 32 °C [34] and 44 °C.[35] The molecular weights of all entries were rather low and unaffected by the loading ratio, which is typical for this type of reaction and has been attributed by other researchers to chain transfer with trace diol or diacid impurities in the monomers.[18,35] The polymerisation was also performed with the addition of toluene equal in volume to CHO. The resulting B/A ratio for the synthesis of entry 9 was about 3, suggesting that solvent addition can be used to alter the B/A ratio.

Finally, an experiment with tetrahydrofuran (THF) was carried out in the expectation that THF would be incorporated into the polymer as shown in Table 3.[16] Indeed, the copolymerisation using complex **3**: SA : CHO : THF mole ratio of 1 : 100 : 1000 : 2500 gave a polymer product with a THF-to-SA incorporation ratio of 0.40 (Table 3, entry 1). The B/A ratio was also decreased from 4.49 (Table 2, entry 7) to 2.23 indicating that THF can compete with the insertion of CHO to limit the consecutive CHO insertions. The T_g of the polymer was measured to be 34.2 °C significantly lower than the T_g of the polymer (52.9 °C) without THF addition (Table 2, entry 7) as a result of the flexible tetramethylene units from THF. Control experiments were performed without SA or with only THF (Table 3, entries 2 and 3 respectively) resulted in no polymerisation after 3 h at 110 °C. However, homopolymerisation of CHO under the same conditions produced poly(CHO) but with poor control as indicated by high dispersity of 2.09 (Table 3, entry 4). This indicates that the presence of THF could inhibit the propagation of CHO to poly(CHO).

Polymer sequence analysis

In order to confirm that the polymers are indeed composed of insertions of SA alternating with multiple insertions of CHO, polymers samples including those from Table 2 entry 3 (no THF), and from Table 3 entry 1 (with added THF) were hydro-

Table 3 Terpolymerisation of "A" succinic anhydride (SA), "B" cyclohexene oxide (CHO), and "C" tetrahydrofuran (THF) along with comparison with control experiments

Entry	Loading ratio Cat. : SA : CHO : THF	TOF (h^{-1})	Degree of polymerisation A : B : C[a]	B/A ratio[a]	C/A ratio[a]	(AB) fraction[a] (%)	M_n[b] (g mol^{-1})	$Đ$[b]	T_g[c] (°C)
1	1 : 100 : 1000 : 2500	63 (SA)	94 : 210 : 38	2.23	0.40	5.5	6400	1.41	34.2
2	1 : 0 : 1000 : 2500	—	—	—	—	—	—	—	—
3	1 : 0 : 0 : 2500	—	—	—	—	—	—	—	—
4	1 : 0 : 1000 : 0	41 (CHO)	0 : 618 : 0	—	—		14 200	2.09	64.4

All experiments were performed using complex **3** for 3 h at 110 °C. Ratios are in molar equivalent. [a] Calculated from NMR spectroscopy, details in the ESI.† [b] Determined by GPC. [c] Determined by DSC.

lysed in aqueous NaOH and THF. NMR spectrometry confirmed the hydrolysis was complete through the absence of ester linkages. A mixture of ether fragments was extracted from the hydrolysis products and then analysed through electrospray ionisation mass spectrometry (ESI-MS). This technique is a non-destructive method of qualitative analysis; though it is unsuitable for determining exact quantities, it can still indicate which species are more common in each sample. From Fig. 5a, it is clearly observed that fragments originating from 4 CHO units form the most common component in the hydrolysed product of the polymer from Table 2, entry 3 in which B/A ratio of 4.14 was observed. For a shorter CHO segment such as in Table 2, entry 9, the ESI-MS after hydrolysis experiment clearly showed the 3 CHO units as the major peak at 335.2 Da (Fig. S19†) in good agreement of the B/A ratio of 3.09.

ESI-MS after hydrolysis for polymer in Table 3, entry 1 showed that most units in the terpolymer are ABBC (major), ABBB, or ABBBB (Fig. 5b) in agreement with the B/A ratio of 2.23. There is an absence of any signal for BC unit. This confirms our results that that there is no ABC unit found in the polymers. The selectivity for each monomer insertion is therefore highly dependent on the previous monomers. Selectivity for THF is highest after two CHO insertions. Meanwhile, there is still a preference for three or four CHO insertions when THF is not inserted. The proposed reaction pathways are illustrated in Fig. 6. After the first insertion of CHO (B), the next insertion will mostly be CHO since $(AB)_n$ sequences are minor and ABC sequences were not observed. Subsequence insertions can be THF (C) giving ABBC sequences (major). Alternatively, additional CHO units can also be inserted giving AB_n sequences. Both pathways will eventually be concluded by an insertion of succinic anhydride (A) to complete the polymerisation cycles.

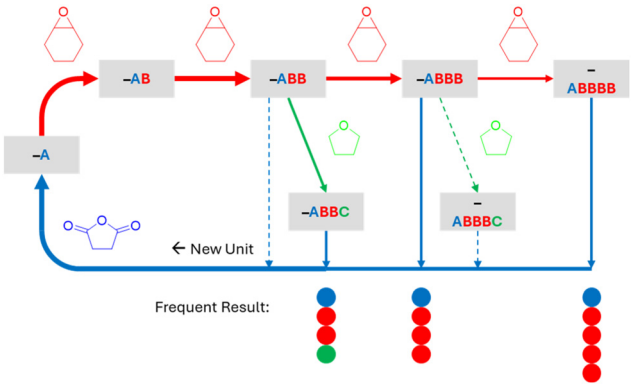

Fig. 6 Monomer insertion pathways for SA, CHO, and THF. Primary pathways shown in solid lines form ABBC, ABBB, and ABBBB units. Secondary pathways are also shown using dashed lines. Uncommon pathways such as for AB units are not shown.

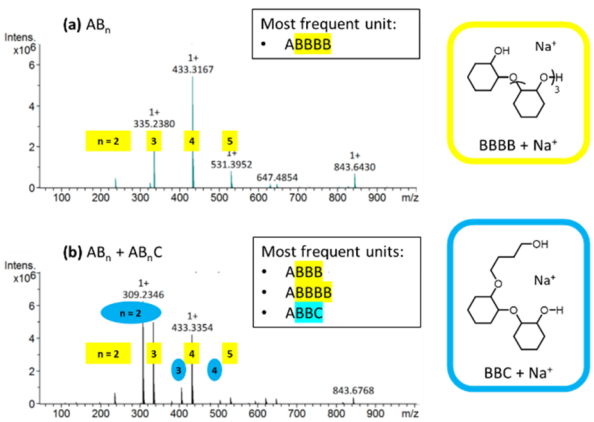

Fig. 5 ESI-MS results for the hydrolysed products of (a) Poly(SA–CHO) and (b) Poly(SA–CHO–THF).

Conclusions

Heteroleptic phenoxyimino tin(II) amides were successfully synthesised and characterized crystallographically. While homoleptic complexes are common, the synthesis of heteroleptic complexes is more challenging since Schlenk equilibrium may exist giving the homoleptic or distribution of both complexes at the end. Therefore, a modified workup procedure was introduced to remove the amine by-product that could facilitate the ligand redistribution process. The tin(II) complexes were used for the copolymerisation between succinic anhydride (A) and cyclohexene oxide (B). Under neat conditions, ABBBB pseudo-periodic polymers could be synthesised. Addition of solvents such as toluene or THF decreased the B/A incorporation ratio. THF (C) could also be

inserted to form ABBC units at a significant proportion. Due to higher ether linkages from multiple insertions of epoxides than the perfectly alternating polymers, this product may then be fine-tuned for tailored properties. This system could augment the potential of the epoxide–anhydride trend by making it possible to tune the incorporation of epoxide monomers. This is advantageous if a particular epoxide monomer is more accessible than the anhydride or is able to confer desirable properties to the product. The terpolymer product from SA, CHO, and THF has a T_g of 34.2 °C. This is an interesting temperature for applications which require softening when in contact with the human body but may be rigid otherwise.

Experimental

Materials and methods

Handling of all chemicals sensitive to oxygen or moisture was performed under a nitrogen atmosphere in a glovebox or with standard Schlenk techniques. Tetrahydrofuran and *n*-hexane were dried by a solvent purification system (MB SPS-800, MBRAUN). Cyclohexene oxide was dried over calcium hydride, distilled under vacuum, and stored at −30 °C in a glovebox. Succinic anhydride was purified by sublimation under vacuum thrice. $Sn[N(SiMe_3)_2]_2$ was synthesised from lithium bis(trimethylsilyl)amide and tin(II) chloride.[36] The phenoxy-imine ligands were synthesised by reacting the appropriate amine with 3,5 di-*tert*-butylsalicylaldehyde.[37,38]

Instrumentation

^{1}H, ^{13}C, and DOSY NMR spectra were recorded on a Bruker AVANCE III HD-600 MHz spectrometer. The NMR solvents used were benzene-d_6 and chloroform-d, which also contained trace non-deuterated impurities suitable for reference as internal standards (C_6D_5H in C_6D_6, δ 7.16 ppm and $CHCl_3$ in $CDCl_3$, δ 7.26 ppm). Single Crystal X-Ray Diffraction (SCXRD) data was collected on a Bruker D8 Venture using a Photon II detector and a Mo Kα radiation (λ = 0.71073 Å) IμS 3.0 microfocus source, accompanied by the Bruker APEX3 software suite. Data integration was performed with the SAINT software, in which the SADABS program was also used to correct intensity data. The space group of each sample was determined using the XPREP software. The crystal structures were solved by a direct method using intrinsic phasing (SHELXT program)[39] and refined by full-matrix least squares against F^2 using the program SHELXL[40] within the Olex2 software package.[41] Anisotropic refinement was applied to all non-H atoms, while the H atoms were placed in calculated positions. Finally, the crystallographic images were processed through the Ortep3 program.[42] GPC analyses were performed on a Malvern Viscotek TDAmax with a refractive index detector as well as a viscometer with two 300 mm × 8.0 mm ID columns packed with a porous styrene divinylbenzene copolymer. Samples were eluted using tetrahydrofuran at a flow rate of 1.0 mL min^{-1} and at 35 °C. Polymer molecular weights and dispersities were calculated using a conventional method. Differential scanning calorimetry (DSC) was carried out using a PerkinElmer DSC-8500 over a temperature range from 0 °C to 100 °C at a heating rate of 20 °C min^{-1} and a gas flow rate of 20 mL min^{-1} under a nitrogen atmosphere. The second heating curve was used to analyse the glass-transition temperature (T_g) of polymer samples. Electro-Spray Ionisation Mass Spectrometry (ESI-MS) was performed using a Bruker Data Analysis Esquire-LC mass spectrometer in ESI mode.

General synthesis of complexes 1–6

The complexes were synthesised in batches. 0.500 mmol of each phenoxy-imine ligand precursor was dissolved in hexane and added to a slight excess of 0.501 mmol tin hexamethyldisilazide. The reaction was complete within two hours. A three-step method was used to extract the complexes: first, most of the hexane solvent was removed *via* vacuum such that the product precipitated but not completely dry. Next, the product was washed with cold hexane to remove most of the HMDS by-product. Finally, the remaining volatiles were removed under vacuum without stirring giving the heteroleptic tin(II) amide complexes in moderate to good yields.

Complex 1. ^{1}H NMR (600 MHz, C_6D_6) δ 7.62 (d, J = 2.7 Hz, 1H, Ar*H*), 7.39 (s, 1H, C*H*=N), 7.00 (d, J = 4.3 Hz, 4H, Ar*H*), 6.88 (hept, J = 4.0 Hz, 1H, Ar*H*), 6.67 (d, J = 2.6 Hz, 1H, Ar*H*), 1.53 (s, 9H, CH_3), 1.20 (s, 9H, CH_3), 0.26 (s, 18H, CH_3). ^{13}C{^{1}H} NMR (151 MHz, C_6D_6) δ 167.73 (*C*H=N), 163.12, 148.11, 142.66, 138.66, 132.36, 130.67, 129.87, 128.22, 128.06, 127.90, 127.47, 122.58, 120.64 (C_{Ar}), 35.54, 34.11 (Ar–*C*), 31.51, 30.22 (*C*H$_3$), 6.18 (Si–*C*H$_3$). Elemental analysis found: C, 55.0; H, 7.68; N, 4.56%. Calculated for $C_{27}H_{44}N_2OSi_2Sn$: C, 55.20; H, 7.55; N, 4.77%. Yield: 197 mg, 67%.

Crystal data for ***1****.* $C_{27}H_{44}N_2OSi_2Sn$, M = 587.51, triclinic, a = 9.5233 (6), b = 12.0193 (8), c = 14.3481 (10) Å, U = 1468.90 (17) Å^3, T = 100 K, space group $P\bar{1}$, Z = 2, 55 801 reflections measured, 7602 unique (R^{int} = 0.047). The final w$R(F^2)$ was 0.080 (all data). Translucent red crystals of **1** were plate-like in shape and obtained from a solution containing the substrate, hexane, and HMDS as hexane evaporated at 300 K. CCDC 2378870.†

Complex 2. ^{1}H NMR (600 MHz, C_6D_6) δ 7.74 (d, J = 2.7 Hz, 1H, Ar*H*), 7.24 (s, 1H, C*H*=N), 6.96 (d, J = 7.5 Hz, 1H, Ar*H*), 6.90 (t, J = 7.5 Hz, 1H, Ar*H*), 6.81 (d, J = 7.6 Hz, 1H, Ar*H*), 6.66 (d, J = 2.7 Hz, 1H, Ar*H*), 2.33 (s, 3H, CH_3), 1.93 (s, 3H, CH_3), 1.65 (s, 9H, CH_3), 1.27 (s, 9H, CH_3), 0.28 (s, 18H, CH_3). ^{13}C{^{1}H} NMR (151 MHz, C_6D_6) δ 170.68 (*C*H=N), 162.57, 146.86, 142.62, 138.67, 132.34, 132.26, 130.91, 130.69, 129.40, 128.75, 127.05, 120.06 (C_{Ar}), 35.57, 34.12 (Ar–*C*), 31.51, 30.25 (*C*H$_3$), 20.02, 19.32 (Ar–*C*H$_3$), 6.20. Elemental analysis found: C, 56.20; H, 7.75; N, 4.43%. Calculated for $C_{29}H_{48}N_2OSi_2Sn$: C, 56.60; H, 7.86; N, 4.55%. Yield: 139 mg, 44%.

Crystal data for ***2****.* $C_{29}H_{48}N_2OSi_2Sn$, M = 615.56, triclinic, a = 10.5871 (13), b = 12.1261 (14), c = 13.7342 (17) Å, U = 1596.4 (3) Å^3, T = 100 K, space group $P\bar{1}$, Z = 2, 65 884 reflections measured, 9325 unique (R^{int} = 0.028). The final w$R(F^2)$ was 0.046 (all data). Translucent yellow crystals of **2** were needle-like in shape and obtained from a solution containing the sub-

strate, hexane, and HMDS as hexane evaporated at 300 K. CCDC 2378871.†

Complex 3. ^{1}H NMR (600 MHz, C_6D_6) δ 7.79 (s, 1H, C*H*═N), 7.73 (d, J = 2.6 Hz, 1H, Ar*H*), 7.14 (d, J = 7.7 Hz, 1H, Ar*H*), 7.09 (t, J = 7.7 Hz, 1H, Ar*H*), 7.02 (d, J = 7.0 Hz, 1H, Ar*H*), 6.84 (d, J = 2.6 Hz, 1H, Ar*H*), 3.66–3.58 (m, C*H*), 3.14–3.05 (m, 1H, C*H*), 1.63 (s, 9H, CH_3), 1.40 (d, J = 6.8 Hz, 3H, CH_3), 1.23 (s, 9H, CH_3), 1.18 (d, J = 6.8 Hz, 3H, CH_3), 1.01 (d, J = 6.8 Hz, 3H, CH_3), 0.85 (d, J = 6.7 Hz, 3H, CH_3), 0.33 (s, 18H, CH_3). ^{13}C{^{1}H} NMR (151 MHz, C_6D_6) δ 171.45 (*C*H═N), 163.00, 144.60, 143.03, 142.44, 141.54, 139.31, 132.58, 130.48, 127.76, 124.35, 124.33, 120.00 (C_{Ar}), 35.57, 34.04 (Ar–*C*), 31.40, 30.21 (*C*H_3), 29.35, 28.28 (Ar–*C*), 26.32, 25.43, 23.18, 22.95 (*C*H_3), 6.63 (Si–*C*H_3). Elemental analysis found: C, 58.70; H, 8.36; N, 4.05%. Calculated for $C_{33}H_{56}N_2OSi_2Sn$: C, 59.00; H, 8.40; N, 4.17%. Yield: 122 mg, 36%.

Crystal data for ***3****.* $C_{33}H_{56}N_2OSi_2Sn$, M = 671.66, monoclinic, a = 10.6210 (13), b = 18.034 (2), c = 18.943 (2) Å, U = 3578.7 (7) Å^3, T = 100 K, space group $P2_1/n$, Z = 4, 233 627 reflections measured, 11 018 unique (R^{int} = 0.035). The final w$R(F^2)$ was 0.047 (all data). Translucent orange crystals of **3** were plate-like in shape and obtained by standing a solution containing the substrate, hexane, and HMDS at 240 K for 24 hours. CCDC 2378872.†

Complex 4. ^{1}H NMR (600 MHz, C_6D_6) δ 7.74 (d, J = 2.6 Hz, 1H, Ar*H*), 7.39 (d, J = 8.2 Hz, 2H, Ar*H*), 7.35 (s, 1H, C*H*═N), 6.96 (d, J = 8.1 Hz, 2H, Ar*H*), 6.81 (d, J = 2.6 Hz, 1H, Ar*H*), 1.61 (s, 9H, CH_3), 1.30 (s, 9H, CH_3), 0.31 (s, 18H, CH_3). ^{13}C{^{1}H} NMR (151 MHz, C_6D_6) δ 168.49 (*C*H═N), 163.64, 150.97, 142.94, 139.03, 133.14, 130.76, 127.08, 127.05, 123.05, 120.43 (C_{Ar}, possible overlap with solvent), 35.53, 34.13 (Ar–*C*), 31.44, 30.17 (*C*H_3), 6.11 (Si–*C*H_3). Elemental analysis found: C, 51.70; H, 6.85; N, 4.00%. Calculated for $C_{28}H_{43}F_3N_2OSi_2Sn$: C, 51.30; H, 6.61; N, 4.27%. Yield: 202 mg, 62%.

Crystal data for ***4****.* $2(C_{28}H_{43}F_3N_2OSi_2Sn)$, M = 1311.02, monoclinic, a = 21.5900 (19), b = 21.3852 (17), c = 14.0681 (13) Å, U = 6364.3 (10) Å^3, T = 100 K, space group $P2_1/c$, Z = 4, 289 330 reflections measured, 12 556 unique (R^{int} = 0.047). The final w$R(F^2)$ was 0.058 (all data). Translucent red crystals of **4** were plate-like in shape and obtained from a solution containing the substrate, hexane, and HMDS as hexane evaporated at 300 K. CCDC 2378873.†

Complex 5. ^{1}H NMR (600 MHz, C_6D_6) δ 7.73 (d, J = 2.6 Hz, 1H, Ar*H*), 7.61 (s, 1H, C*H*═N), 7.30 (d, J = 8.3 Hz, 2H, Ar*H*), 7.15 (d, overlaps with solvent, 2H, Ar*H*), 6.83 (d, J = 2.6 Hz, 1H, Ar*H*), 1.65 (s, 9H, CH_3), 1.30 (s, 9H, CH_3), 1.20 (s, 9H, CH_3), 0.37 (s, 18H, CH_3). ^{13}C{^{1}H} NMR (151 MHz, C_6D_6) δ 167.33 (*C*H═N), 163.04, 150.79, 145.68, 142.66, 138.63, 132.20, 130.55, 126.83, 122.29, 120.74 (C_{Ar}), 35.56, 34.63, 34.11 (Ar–*C*), 31.52, 31.34, 30.25 (*C*H_3), 6.18 (Si–*C*H_3). Elemental analysis found: C, 58.10; H, 8.05; N, 4.55%. Calculated for $C_{31}H_{52}N_2OSi_2Sn$: C, 57.85; H, 8.10; N, 4.35%. Yield: 223 mg, 69%.

Crystal data for ***5****.* $C_{31}H_{52}N_2OSi_2Sn$, M = 643.61, monoclinic, a = 9.9746 (13), b = 27.777 (3), c = 12.2977 (15) Å, U = 3407.2 (7) Å^3, T = 100 K, space group $P2_1/c$, Z = 4, 60 650 reflections measured, 7850 unique (R^{int} = 0.085). The final w$R(F^2)$ was 0.110 (all data). Translucent orange-red crystals of **5** were chunky in shape and obtained by standing a solution containing the substrate, dichloromethane, hexane, and HMDS at 300 K for two weeks. CCDC 2378874.†

Complex 6. ^{1}H NMR (600 MHz, C_6D_6) δ 7.72 (d, J = 2.7 Hz, 1H, Ar*H*), 7.60 (s, 1H, C*H*═N), 7.21–7.11 (m, 2H, Ar*H*), 6.82 (d, J = 2.6 Hz, 1H, Ar*H*), 6.80–6.76 (m, 2H, Ar*H*), 3.25 (s, 3H, CH_3), 1.65 (s, 9H, CH_3), 1.31 (s, 9H, CH_3), 0.41 (s, 18H, CH_3). ^{13}C{^{1}H} NMR (151 MHz, C_6D_6) δ 166.71 (*C*H═N), 162.91, 159.57, 142.60, 141.17, 138.65, 132.03, 130.53, 123.74, 120.73, 115.16, 55.13 (O–*C*H_3), 35.56, 34.12 (*C*H_3), 31.54, 30.25 (*C*H_3), 6.24 (Si–*C*H_3). Elemental analysis found: C, 54.70; H, 7.20; N, 4.46%. Calculated for $C_{28}H_{46}N_2O_2Si_2Sn$: C, 54.50; H, 7.50; N, 4.54%. Yield: 138 mg, 45%.

Crystal data for ***6****.* $C_{28}H_{46}N_2O_2Si_2Sn$, M = 617.54, monoclinic, a = 10.5296 (8), b = 9.2642 (7), c = 31.659 (3) Å, U = 3078.7 (4) Å^3, T = 100 K, space group $P2_1/c$, Z = 4, 92 618 reflections measured, 6075 unique (R^{int} = 0.124). The final w$R(F^2)$ was 0.051 (all data). Translucent red crystals of **6** were plate-like in shape and obtained by standing a solution containing the substrate, hexane, dichloromethane, and HMDS at 240 K for 24 hours. CCDC 2378875.†

Polymerisation procedure

Polymerisation was carried out under N_2 atmosphere using glovebox or Schlenk techniques. In one example, 0.0100 mmol (6.72 mg) of complex **3** was added to a polymerisation flask charged with 2.00 mmol (200 mg) of SA and 10.0 mmol (1.01 ml) of CHO. The polymerisation was carried out in an oil bath at 110 °C and stirred *via* magnetic bar. Reactions were generally stopped before very high conversions due to the neat reaction mixture becoming viscous. After polymerisation, a small crude sample was taken for NMR analysis. Subsequently, a small quantity of dichloromethane was added to the crude product and the mixture was precipitated in excess cold methanol. After separation *via* centrifuge, the polymer was dried at 50 °C under vacuum. The polymer samples were also analysed by NMR for compositions and other parameters. Please see ESI† for more details.

Warning: Terpolymerisation and control experiments involving THF were performed in a stainless-steel reactor to accommodate the increase in pressure as the experiment temperature (110 °C) is well above the boiling point of THF (66 °C).

Polymer hydrolysis

Polymer samples were hydrolysed under basic conditions. For each, a vial was charged with 50 mg of polymer, 1 ml of THF, and 1 ml of aqueous NaOH (4 M). The biphasic mixture was stirred at 50 °C for 48 hours. Afterwards, the mixture was then acidified with 2 ml of aqueous HCl (4 M). Then, most of the THF fraction was removed with a vacuum rotary evaporator and the hydrolysed products were extracted with ethyl acetate (3 × 2 ml). The combined organic phase was dried over sodium carbonate and ethyl acetate removed by vacuum. The sample was then dissolved in a 1 : 1 solution of ethyl acetate

and ethanol and analysed through ESI-MS, a low energy and non-destructive technique.

Data availability

The data supporting this article have been included as part of the ESI.†

Conflicts of interest

There are no conflicts to declare.

Acknowledgements

Financial support from Vidyasirimedhi Institute of Science and Technology (M22KHP-VIS010) and National Research Council of Thailand (NRCT) (no. N42 A650196) are gratefully acknowledged. The authors also acknowledge financial support from the Thailand Science Research and Innovation (FRB680014/0457) and Program Management Unit for Human Resources & Institutional Development, Research and Innovation (grant number: B41G680026, Global League). Support for scientific instruments from Frontier Research Center, VISTEC, is gratefully acknowledged.

References

1 J. M. Longo, M. J. Sanford and G. W. Coates, *Chem. Rev.*, 2016, **116**, 15167–15197.
2 X. Wang, Z. Huo, X. Xie, N. Shanaiah and R. Tong, *Chem. – Asian J.*, 2023, **18**, e202201147.
3 G. Capiel, J. Uicich, D. Fasce and P. E. Montemartini, *Polym. Degrad. Stab.*, 2018, **153**, 165–171.
4 Y. Tokiwa, B. P. Calabia, C. U. Ugwu and S. Aiba, *Int. J. Mol. Sci.*, 2009, **10**, 3722–3742.
5 C. Romain, Y. Zhu, P. Dingwall, S. Paul, H. S. Rzepa, A. Buchard and C. K. Williams, *J. Am. Chem. Soc.*, 2016, **138**, 4120–4131.
6 Y. Zhou, C. Hu, T. Zhang, X. Xu, R. Duan, Y. Luo, Z. Sun, X. Pang and X. Chen, *Macromolecules*, 2019, **52**, 3462–3470.
7 Y. Xia and J. Zhao, *Polymer*, 2018, **143**, 343–361.
8 A. Kummari, S. Pappuru and D. Chakraborty, *Polym. Chem.*, 2018, **9**, 4052–4062.
9 A. Takasu, M. Ito, Y. Inai, T. Hirabayashi and Y. Nishimura, *Polym. J.*, 1999, **31**, 961–969.
10 F. Isnard, M. Carratù, M. Lamberti, V. Venditto and M. Mazzeo, *Catal. Sci. Technol.*, 2018, **8**, 5034–5043.
11 R. C. Jeske, A. M. DiCiccio and G. W. Coates, *J. Am. Chem. Soc.*, 2007, **129**, 11330–11331.
12 E. Hosseini Nejad, C. G. W. van Melis, T. J. Vermeer, C. E. Koning and R. Duchateau, *Macromolecules*, 2012, **45**, 1770–1776.
13 H. Li, G. He, Y. Chen, J. Zhao and G. Zhang, *ACS Macro Lett.*, 2019, **8**, 973–978.
14 H. L. Hsieh, *J. Macromol. Sci., Part A: Pure Appl. Chem.*, 1973, **7**, 1525–1535.
15 T. Tang, M. Oshimura, S. Yamada, A. Takasu, X. Yang and Q. Cai, *J. Polym. Sci., Part A: Polym. Chem.*, 2012, **50**, 3171–3183.
16 N. Jabprakon, P. Chumsaeng and K. Phomphrai, *Polym. Chem.*, 2023, **14**, 4169–4181.
17 R. W. F. Kerr and C. K. Williams, *J. Am. Chem. Soc.*, 2022, **144**, 6882–6893.
18 R. W. F. Kerr, A. R. Craze and C. K. Williams, *Chem. Sci.*, 2024, **15**, 11617–11625.
19 V. K. Chidara, Y. Gnanou and X. Feng, *Molecules*, 2022, **27**, 466.
20 Y. Takahashi, A. Kanazawa and S. Aoshima, *Macromolecules*, 2023, **56**, 4198–4207.
21 T. Ungpittagul, T. Jaenjai, T. Roongcharoen, S. Namuangruk and K. Phomphrai, *Macromolecules*, 2020, **53**, 9869–9877.
22 N. Yuntawattana, G. L. Gregory, L. P. Carrodeguas and C. K. Williams, *ACS Macro Lett.*, 2021, **10**, 774–779.
23 L. Wang, C. E. Kefalidis, S. Sinbandhit, V. Dorcet, J.-F. Carpentier, L. Maron and Y. Sarazin, *Chem. – Eur. J.*, 2013, **19**, 13463–13478.
24 N. Nimitsiriwat, V. C. Gibson, E. L. Marshall, A. J. P. White, S. H. Dale and M. R. J. Elsegood, *Dalton Trans.*, 2007, 4464–4471.
25 K. Phomphrai, C. Pongchan-o, W. Thumrongpatanaraks, P. Sangtrirutnugul, P. Kongsaeree and M. Pohmakotr, *Dalton Trans.*, 2011, **40**, 2157–2159.
26 N. Nimitsiriwat, V. C. Gibson, E. L. Marshall and M. R. J. Elsegood, *Dalton Trans.*, 2009, 3710–3715.
27 N. Nimitsiriwat, E. L. Marshall, V. C. Gibson, M. R. J. Elsegood and S. H. Dale, *J. Am. Chem. Soc.*, 2004, **126**, 13598–13599.
28 P. Piromjitpong, P. Ratanapanee, W. Thumrongpatanaraks, P. Kongsaeree and K. Phomphrai, *Dalton Trans.*, 2012, **41**, 12704–12710.
29 J. D. Parish, M. W. Snook, A. L. Johnson and G. Kociok-Köhn, *Dalton Trans.*, 2018, **47**, 7721–7729.
30 J. D. Parish, M. W. Snook and A. L. Johnson, *Dalton Trans.*, 2021, **50**, 13902–13914.
31 A. Walsh, D. J. Payne, R. G. Egdell and G. W. Watson, *Chem. Soc. Rev.*, 2011, **40**, 4455–4463.
32 A. Kleawkla, R. Molloy, W. Naksata and W. Punyodom, *Adv. Mater. Res.*, 2008, **55–57**, 757–760.
33 A. P. Dove, V. C. Gibson, E. L. Marshall, H. S. Rzepa, A. J. P. White and D. J. Williams, *J. Am. Chem. Soc.*, 2006, **128**, 9834–9843.
34 L. Lin, J. Liang, Y. Xu, S. Wang, M. Xiao, L. Sun and Y. Meng, *Green Chem.*, 2019, **21**, 2469–2477.
35 M. Martínez de Sarasa Buchaca, F. de la Cruz-Martínez, J. Martínez, C. Alonso-Moreno, J. Fernández-Baeza, J. Tejeda, E. Niza, J. A. Castro-Osma, A. Otero and A. Lara-Sánchez, *ACS Omega*, 2018, **3**, 17581–17589.

36 M. J. S. Gynane, D. H. Harris, M. F. Lappert, P. P. Power, P. Rivière and M. Rivière-Baudet, *J. Chem. Soc., Dalton Trans.*, 1977, 2004–2009.
37 S. Kigoshi, A. Kanazawa, S. Kanaoka and S. Aoshima, *J. Polym. Sci., Part A: Polym. Chem.*, 2019, **57**, 2021–2029.
38 P. A. Cameron, V. C. Gibson, C. Redshaw, J. A. Segal, G. A. Solan, A. J. P. White and D. J. Williams, *J. Chem. Soc., Dalton Trans.*, 2001, 1472–1476.
39 G. Sheldrick, *Acta Crystallogr., Sect. A: Found. Adv.*, 2015, **71**, 3–8.
40 G. Sheldrick, *Acta Crystallogr., Sect. C: Struct. Chem.*, 2015, **71**, 3–8.
41 O. V. Dolomanov, L. J. Bourhis, R. J. Gildea, J. A. K. Howard and H. Puschmann, *J. Appl. Crystallogr.*, 2009, **42**, 339–341.
42 L. Farrugia, *J. Appl. Crystallogr.*, 2012, **45**, 849–854.